© 2020. Published by The Company of Biologists Ltd | Journal of Experimental Biology (2020) 223, jeb218974. doi:10.1242/jeb.218974

RESEARCH ARTICLE

Thermo-TRPs and gut microbiota are involved in thermogenesis and energy metabolism during low temperature exposure of obese mice

Jing Wen[1,2,*], Tingbei Bo[1,2,*], Xueying Zhang[1,2], Zuoxin Wang[3] and Dehua Wang[1,2,‡]

ABSTRACT

Ambient temperature and food composition can affect energy metabolism of the host. Thermal transient receptor potential ion channels (thermo-TRPs) can detect temperature signals and are involved in the regulation of thermogenesis and energy homeostasis. Further, the gut microbiota have also been implicated in thermogenesis and obesity. In the present study, we tested the hypothesis that thermo-TRPs and gut microbiota are involved in reducing diet-induced obesity (DIO) during low temperature exposure. C57BL/6J mice in obese (body mass gain >45%), lean (body mass gain <15%) and control (body mass gain <1%) groups were exposed to high (23±1°C) or low (4±1°C) ambient temperature for 28 days. Our data showed that low temperature exposure attenuated DIO, but enhanced brown adipose tissue (BAT) thermogenesis. Low temperature exposure also resulted in increased noradrenaline (NA) concentrations in the hypothalamus, decreased TRP melastatin 8 (TRPM8) expression in the small intestine, and altered composition and diversity of gut microbiota. In DIO mice, there was a decrease in overall energy intake along with a reduction in TRP ankyrin 1 (TRPA1) expression and an increase in NA concentration in the small intestine. DIO mice also showed increases in *Oscillospira*, [*Ruminococcus*], *Lactococcus* and *Christensenella* and decreases in *Prevotella*, *Odoribacter* and *Lactobacillus* at the genus level in fecal samples. Together, our data suggest that thermos-TRPs and gut microbiota are involved in thermogenesis and energy metabolism during low temperature exposure in DIO mice.

KEY WORDS: Low temperature exposure, Gut microbiota, Obesity, Thermogenesis, Thermal transient receptor potential

INTRODUCTION

Obesity is a common condition accompanied by a series of metabolic disorders (Ley et al., 2005; Nudel and Sanchez, 2019). Chronic energy intake that exceeds energy expenditure leads to energy accumulation, which has been considered a main driver of obesity (Romieu et al., 2017; Yoo et al., 2014). Intake of high-fat food can quickly cause fat accumulation. Conversely, low temperature exposure can increase thermogenesis in brown adipocytes of mice, rats, hamsters and humans, and attenuate obesity (Saito et al., 2015; Rothwell and Stock, 1979; Suárez-Zamorano et al., 2015; Ziętak et al., 2016).

Low temperature exposure in small mammals typically results in behavioral and physiological responses that minimize heat dissipation (e.g. vasoconstriction, huddling) and increase heat production [e.g. shivering, non-shivering thermogenesis (NST)] (Bo et al., 2019; Hoffstaetter et al., 2018; Ravussin et al., 2014). In addition, low temperature exposure can promote adrenergic release from sympathetic nerves in brown adipose tissue (BAT), which, in turn, can be activated by noradrenaline (NA) stimulation (Rossato et al., 2014). Activation of this pathway can stimulate uncoupling protein 1 (UCP1), increase the capacity of NST and decrease energy accumulation (Cannon and Nedergaard, 2004; Li et al., 2019a). It has been shown that low temperatures can be sensed by transient receptor potential melastatin 8 (TRPM8) and/or ankyrin 1 (TRPA1), both of which are expressed in peripheral cutaneous nerve endings. Their activations can induce adrenergic release, thereby activating BAT thermogenesis (Bachman et al., 2002; Barbatelli et al., 2010).

The TRP multigene superfamily has eight sub-families (Li, 2017) and is expressed in almost all tissue, including BAT and the small intestine (Nilius and Owsianik, 2011). As non-selective cation channels, TRPs can be activated by temperature and are involved in regulating thermogenesis and energy homeostasis (Señarís et al., 2018; Song et al., 2016; Vay et al., 2012). Low temperatures are mainly sensed by TRPM8 and TRPA1, which are activated by temperatures below 28°C and 17°C, respectively (Bödding et al., 2007). Moreover, TRPM8 and TRPA1 participate in BAT thermogenesis activation induced by low temperature exposure (Saito et al., 2015) and enhance energy metabolism in mice (Uchida et al., 2017). TRPM8 is expressed in brown adipocytes and can increase UCP1 expression and heat production (Ma et al., 2012; Rossato et al., 2014). Although the thermo-sensation of TRPA1 remains controversial, recent data have shown that TRPA1 takes part in energy homeostasis, including glucose homeostasis (Señarís et al., 2018). These two thermo-TRPs have been considered as potential therapeutic targets for preventing and treating obesity and its related metabolic disorders.

Recently, the gut microbiota have been implicated in the regulation of energy homeostasis and body mass (Tremaroli and Bäckhed, 2012). The gut microbiota affect DIO via different pathways involved in triglyceride storage and fatty acid oxidation (Bäckhed et al., 2007). Obesity is found to be associated with changes in microbial diversity and relative proportions between the Firmicutes and Bacteroidetes phyla in both mice and humans (Ley et al., 2005, 2006; Turnbaugh et al., 2008). Transplantation of caecal contents from cold-exposed mice can significantly reduce obesity and improve insulin sensitivity in the host (Chevalier et al., 2015). Data have also shown that germ-free mice have impaired thermogenesis of BAT, which is associated with limited increases in UCP1 expression and reduced browning of

[1]State Key Laboratory of Integrated Management of Pest Insects and Rodents, Institute of Zoology, Chinese Academy of Sciences, Beijing 100101, China. [2]CAS Center for Excellence in Biotic Interactions, University of Chinese Academy of Sciences, Beijing 100049, China. [3]Department of Psychology and Program in Neuroscience, Florida State University, Tallahassee, FL 32306-1270, USA.
*These authors contributed equally to this work

‡Author for correspondence (wangdh@ioz.ac.cn)

J.W., 0000-0002-5212-1053; D.W., 0000-0002-7322-2371

Received 25 November 2019; Accepted 17 April 2020

Journal of Experimental Biology (2020) 223, jeb218974. doi:10.1242/jeb.218974

white adipose tissue (WAT) (Bo et al., 2019; Li et al., 2019a). Collectively, these data suggest that both BAT and gut microbiota contribute to thermogenesis and inhibition of obesity at low temperature. Recent studies have also linked changes in the gut microbiota in cold environments to the thermogenesis of BAT via exogenous NA (Bo et al., 2019), bile acid (Ziętak et al., 2016) and butyric acid (Li et al., 2019b). However, it remains unclear how gut microbiota in the small intestine perceive temperature signals.

The aim of the present study was to illustrate a gut microbial signature for obese mice under low temperature, to explore the mechanisms by which intestinal cells or gut microbiota sense the host environment and the animal's physiological changes, and to reveal the possible relationship between gut microbiota and TRPs in thermogenesis and metabolism. We hypothesized that TRPs play an important role in attenuating DIO during low temperature exposure by sensing ambient temperature and are also involved in regulating metabolism and changes in gut microbiota composition and structure.

MATERIALS AND METHODS

Animals

In total, 85 C57BL/6J male mice (5 weeks old, 22.0–28.0 g) were housed individually in plastic cages (29×18×16 cm) with sawdust bedding in a temperature-controlled room (23±1°C), under a 16 h:8 h light:dark cycle (lights on at 04:00 h). Water and standard rodent chow (6.2% fat, 35.6% carbohydrate, 20.8% protein and 17.6 gross energy kJ g^{-1}) (Beijing Keao Xieli Feed Co., China) or high-fat food (60% fat, 20% carbohydrate, 20% protein, and 22.0 gross energy kJ g^{-1}) (Research Diet Inc., D12492, USA) were provided *ad libitum*. The animal procedures were approved by the Animal Care and Use Committee of the Institute of Zoology, Chinese Academy of Sciences (CAS).

Experimental design

The mice were acclimated at 23±1°C for 3 weeks. Thereafter, 10 animals were randomly chosen to be in the control group and fed standard rodent chow. The remaining animals were fed high-fat food for 8 weeks. By the end of the 8 weeks, all animals fed with high-fat food were rank-ordered by their body mass. Fourteen animals from both the low and high ends of body mass measurements were assigned as either lean (body mass gain less than 15%) or obese (body mass gain more than 45%) groups. Fat is a key grouping factor which refers to different foods and body mass. Significant differences were found in body mass between control (29.24±0.60 g), lean (33.31±0.53 g) and obese (42.54±1.17 g) groups ($F_{2,36}$=57.70, P<0.0001). Mice within each group were subsequently and randomly assigned to be exposed to either 23°C or 4°C ambient temperature (T_a) for 4 weeks. In total, six experimental groups with the combination of temperature and degree of obesity were created: 23°C–control (n=5), 4°C–control (n=5), 23°C–obese (n=7), 4°C–obese (n=7), 23°C–lean (n=7) and 4°C–lean (n=7).

Body mass and gross energy intake (GEI)

Body mass of the mice were measured at 18:00 h each day. Daily food intake was calculated as the mass of food offered minus food remained in the hopper and food mixed in the bedding. The gross energy content of the food was then determined using a C2000 oxygen bomb calorimeter (PARR 1281, USA) and GEI was calculated as follows:

$$\text{GEI} = \text{dry matter intake} \times \text{energy content}, \quad (1)$$

where GEI is in kJ day^{-1}, dry matter intake is in g day^{-1} and energy content is in kJ g^{-1}.

Temperature preference

The apparatus consisted of two plastic cages (35×25×20 cm) with one cage filled with ice while the other cage remained empty. The two cages were placed next to each other, separated by a board of polyethylene foam, and covered with an opaque plastic plate. The room temperature was maintained at 23±1°C. Subjects were placed in the middle line of the plastic plate and allowed to roam freely. After 5 min of acclimation, the subject's time spent in each area of the plate was recorded for 10 min. The duration of time spent on the cold surface (above the ice cage) was used as an index of cold tolerance.

Glucose tolerance test (GTT)-glycemia

Mice were fasted for 12 h before the intraperitoneal injection of 20% glucose solution (2 mg g^{-1} body mass). Blood was collected from the tail vein to determine blood glucose levels, which were measured at baseline, 15, 30, 60 and 120 min after glucose injection by using a blood glucose meter (the USA, model: FreeStyle Freedom Lite) and test paper.

Resting metabolic rate (RMR) and non-shivering thermogenesis (NST)

RMR and maximum non-shivering thermogenesis (NSTmax) were estimated by measuring the rate of oxygen consumption using an open-flow respirometry system (TSE, Germany) at the end of the 4-week temperature exposure. After drying, air was pumped at a rate of 1000 ml min^{-1} through a cuboid sealed Perspex chamber. Gas leaving the chamber was dried using a special drier (TSE system, Germany) and passed through an oxygen analyzer at a flow rate of 380 ml min^{-1}. The data were recorded and averaged every 10 s by a computer connected via an analogue-to-digital converter that converted the changes of air composition to digital signal (TSE system, Germany), then analyzed using Labmaster software (TSE system, Germany). The mice had access to food and water prior to the measurements of RMR and NSTmax, during which subjects were deprived of food and water. RMR was measured for 3 h at 30±0.5°C and calculated from the lowest rate of oxygen consumption over 10 min. RMR measurements for all subjects were completed during a 2-day window. The accuracy of the oxygen analysis was checked periodically using the standard gas by an experienced technician.

NSTmax was the maximum rate of oxygen consumption in response to NA and was induced by a subcutaneous injection of NA at 15±0.5°C. The mass-dependent dosage of NA (mg kg^{-1}) was calculated according to the equation: $\text{NA}=6.6M_b^{-0.458}$ (where M_b is body mass in grams) (Heldmaier, 1971). NSTmax was calculated from continuous stable maximal recordings over 10 min. All measurements were performed between 06:00 and 19:00 h during the light phase of the photoperiod.

Body temperature

Rectal temperatures (T_{core}) were recorded by inserting a temperature probe (TES 1310) 3 cm into the rectum daily during the temperature exposure period. At the end of the experiment, surface body temperatures ($T_{surface}$) were read with an infrared camera (FLIR E60, UK) from a distance of 30 cm, and the data were analyzed using FLIR Tools software. The highest temperatures of shell and tail in an image were selected.

Body composition, body fat content and fat volume

Animals were killed between 14:00 and 16:00 h at the end of the experiment. Interscapular BAT, small intestines and brains were quickly excised and immediately frozen in liquid nitrogen following

the collection of trunk blood. Next, the caecum, rectum, stomach, liver, lung and kidneys were separated from the remainder of the carcass and dried in an oven at 60°C to determine dry mass. Total body fat was extracted from the dried carcass by ether extraction in a Soxhlet apparatus (2055 SOXTEC Manual Extraction Unit). The body fat volume was calculated using an *in vivo* imaging system for living animals (small animal CT) (PE Quantum FX).

Short-chain fatty acids (SCFAs)

At the end of experiment, feces were collected from each animal using sterilized tools and were placed into super-clean tubes, frozen immediately in liquid nitrogen and stored at −80°C. Acetic, propionic, butyric, isobutyric, valeric and isovaleric acids in the feces were measured by high-performance gas chromatography (GC, Agilent 7890A, Agilent Technologies, Germany) with a modified GC autosampler and FID system (Zhang et al., 2018). Separations were performed in a 30 m×0.25 mm×0.25 µm DB-WAX column (Agilent Technologies) using 99.998% hydrogen as carrier gas at a flow rate of 1.0 ml min^{-1} (Zhang et al., 2018). The system operated at 250°C. Injections were performed at 230°C in the splitless mode, with 0.5 µl per injection. The oven temperature was programmed from 60°C (1 min) to 200°C at 5°C min^{-1} and then from 200 to 230°C at 10°C min^{-1}. The total running time of each sample was 32 min.

Monoamine neurotransmitters – NA

High performance liquid chromatography with electrochemical detection (HPLC-ECD) was used to measure NA in the small intestine and hypothalamic samples. The 3,4-dihydroxybenzylamine (DHBA) was used as internal standard. Samples were homogenized in 0.1 mol l^{-1} cold perchloric acid, oscillated with ultrasound for 10 s, followed by centrifugation at 13,000 rpm at 4°C for 30 min. Supernatant was filtered using 0.2 mm nylon filter. Aliquots of 30 µl were manually injected using a Hamilton syringe.

Western blot

Western blotting was performed on whole tissue lysates and were probed with the following primary antibodies: UCP1 (ab155117, Abcam), β-tubulin (A01030HRP, Abbkine) and GAPDH (A01020, Abbkine). Anti-TRPA1 (PA1-46159) and Anti-TRPM8 (ab3243) were purchased from Thermo Fisher Scientific and Abcam (UK). The secondary antibodies used were either peroxidase-conjugated goat anti-rabbit IgG (111-035-003, Jackson) or peroxidase-conjugated goat anti-mice IgG (115-035-003, Jackson).

Samples from the small intestine (0.2 g) and BAT (0.2 g) were homogenized in RIPA buffer using established methods (Bo et al., 2019). The total protein was separated by SDS-PAGE using a Mini Protean apparatus (Bio-Rad Laboratories, PA, USA) and transferred onto PVDF membranes, which were then blocked with 5% skimmed milk for 1.5 h at room temperature. Thereafter, the membranes were incubated with the primary antibodies for approximately 12 h at 4°C, followed by incubation with an appropriate horseradish peroxidase-conjugated secondary antibody for 2 h at room temperature. Antibody concentrations were determined based on the literature and our pilot experiments. The reaction products were revealed by chemiluminescence (ECL, Yesen).

Microbiota DNA extraction

DNA from fecal samples were extracted by 2×CTAB (cetyltrimethyl ammonium bromide), phenol chloroform mixture (phenol:chloroform:isoamyl alcohol=25:24:1) and SanPrep Column DNA Gel Extraction Kit (Sangon Biotech, China). DNA purity and concentrations were assessed by absorbance on a Nanodrop 2000 (Thermo Fisher Scientific, Carlsbad, CA, USA) by measuring the A260/A280 ratio. Only DNA with an A260/A280 ratio of 1.8–2.0 was used.

16S rDNA gene sequencing analysis

The 16S sequence paired-end dataset was joined and quality filtered using the FLASH method described by Magoč and Salzberg (2011). Sequencing was done on an Illumina HiSeq 2500. All sequence analyses were provided in the Quantitative Insights Into Microbial Ecology (QIIME, version 1.9.1) software suite according to the Qiime tutorial (http://qiime.org/) with modified methods. Sequences that did not match any entries in this reference were subsequently clustered into *de novo* operational taxonomic units (OTUs) at 97% similarity with UCLUST. The hierarchical clustering on the basis of population profiles of most common and abundant taxa was performed using UPGMA clustering (unweighted pair group method with arithmetic mean, also known as average linkage) on the distance matrix of OTU abundance.

Statistical analysis

SPSS 20.0 software was used for statistical analyses. For intra- and inter-group analyses, repeated-measures ANOVA or two-way ANOVA (fat×T_a) was applied when appropriate, followed by Tukey's *post hoc* test. All data are presented as means±s.e.m., and $P<0.05$ was deemed statistically significant.

For microbiota data, the OTUs that reached a nucleotide similarity level of 97% were used for α-diversity (Shannon). Principal coordinate analyses (PCoA) based on weighted and unweighted UniFrac distances were used to visualize the variation of bacterial structure across different groups using the vegan package in R. Significance for β-diversity analyses was checked with analysis of similarity (ANOSIM) included in the package vegan of the QIIME-incorporated version of R. The linear discriminant analysis (LDA) effect size (LEfSe) method was used to assess differences in microbial communities using an LDA score threshold of 2.The Kyoto Encyclopedia of Genes and Genomes (KEGG) orthologs were used to evaluate the potential functional of gut microbiota. Differences in α-diversity, and phyla and genera abundance were analyzed using two-way ANOVA with Tukey's *post hoc* test.

RESULTS

Energy metabolism

Body mass

There were significant interactions between time (days) and fat ($F_{56,924}=6.656$, $P<0.01$) and time and T_a ($F_{28,924}=11.811$, $P<0.01$), but not between fat and T_a ($F_{2,33}=1.995$, $P>0.05$; Fig. 1A,B). After 4 weeks of exposure to 4°C T_a, mice showed a significant lower body mass gain compared with their counterparts at 23°C ($F_{1,33}=4.915$, $P<0.05$; Fig. 1E). At 4°C, the average body mass in the obese group was significantly lower than the other two groups, which did not differ from each other ($F_{2,33}=35.517$, $P<0.01$; Fig. 1F).

Energy intake

Energy intake changed over time in all experimental groups ($F_{88,924}=2.870$, $P<0.01$; Fig. 1C,D). Mice in the obese group had the lowest average energy intake ($F_{2,33}=5.779$, $P<0.01$; Fig. 1G) compared with the energy intake of the other two groups, which did not differ from each other. In addition, mice at 4°C had a higher average energy intake than mice at 23°C ($F_{1,33}=7.241$, $P<0.05$; Fig. 1G). A significant fat–T_a interaction was also found ($F_{2,33}=5.174$, $P<0.01$).

Journal of Experimental Biology (2020) 223, jeb218974. doi:10.1242/jeb.218974

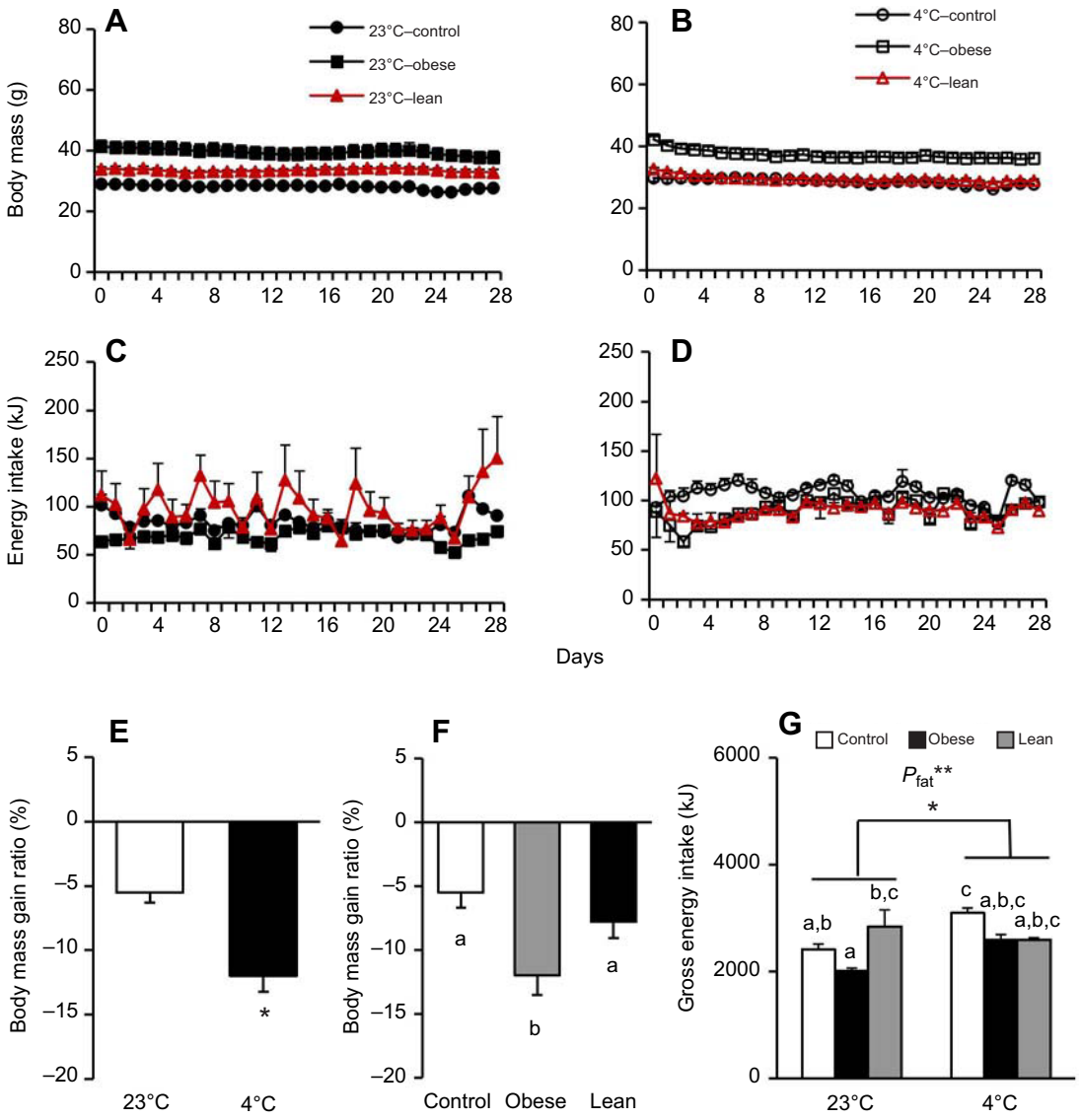

Fig. 1. Diet-induced obesity (DIO) and low temperature exposure affect the body mass and energy intake of C57BL/6J mice. Effects of DIO and low temperature exposure on (A,B) body mass, (C,D) energy intake, (E,F) body mass gain ratio and (G) gross energy in C57BL/6J mice. Data are presented as means ±s.e.m. Different letters indicate significant between-group differences determined by Tukey's *post hoc* tests (P<0.05). P_{fat}**, significant effect of DIO (P<0.01). *P<0.05.

Body fat content and energy metabolism

As shown in Fig. 2A, the obese group had the highest level of body fat content ($F_{2,32}$=82.223, P<0.01), and the lean group also had a higher level of body fat content compared with the control group. In addition, the mice at 23°C showed higher body fat content than those at 4°C ($F_{1,32}$=19.341, P<0.01), and a significant fat–T_a interaction was also found ($F_{2,32}$=3.884, P<0.05). The effects of fat ($F_{2,23}$=1.842, P>0.05), T_a ($F_{1,23}$=1.207, P>0.05) and the fat–T_a interaction ($F_{2,23}$=1.442, P>0.05) on fat volume were not significant (Fig. 2B). The obese group had higher body fat volume than the other groups only at 23°C. RMR ($F_{2,32}$=3.605, P<0.05; Fig. 2C) and GTT-glycemia ($F_{2,32}$=6.203, P<0.01; Fig. 2F) were affected significantly by body fat content. The RMR in the control group did not differ from that of the obese group but was higher than that of the lean group. Conversely, the obese group had higher GTT-glycemia than the other two groups, which did not differ from each other. The level of fasting blood glucose was higher in mice at 23°C than at 4°C ($F_{1,23}$=4.684, P<0.05; Fig. 2E). Relative to 23°C controls, mice at 4°C showed higher NST ($F_{1,33}$=5.238, P<0.05; Fig. 2D) and higher amounts of UCP1 ($F_{1,33}$=4.203, P<0.05; Fig. 2G), which was essential for heat production via adaptive thermogenesis in BAT.

Body temperature and cold tolerance

Rectal temperature was significantly affected by T_a ($F_{1,33}$=10.746, P<0.01; Fig. 3A,B), but not by fat or the fat–T_a interaction ($F_{2,33}$=1.184, 1.486, respectively; both P>0.05). Meanwhile, shell temperature, tail skin temperature and BAT skin temperature were significantly affected by T_a ($F_{1,33}$=54.940, 272.885, 45.196, respectively; all P<0.01) and fat ($F_{2,33}$=10.765, 8.953, 8.922, respectively; all P<0.01) (Fig. 3C–E). Moreover, a significant fat–T_a interaction was found for tail skin temperature ($F_{2,33}$=3.305, P<0.01, Fig. 3D). Compared with mice at 23°C, mice at 4°C had better cold tolerance ($F_{2,24}$=23.615, P<0.01). In particular, mice in the obese group did better than the other two groups at 4°C (Fig. 3F,G).

Journal of Experimental Biology (2020) 223, jeb218974. doi:10.1242/jeb.218974

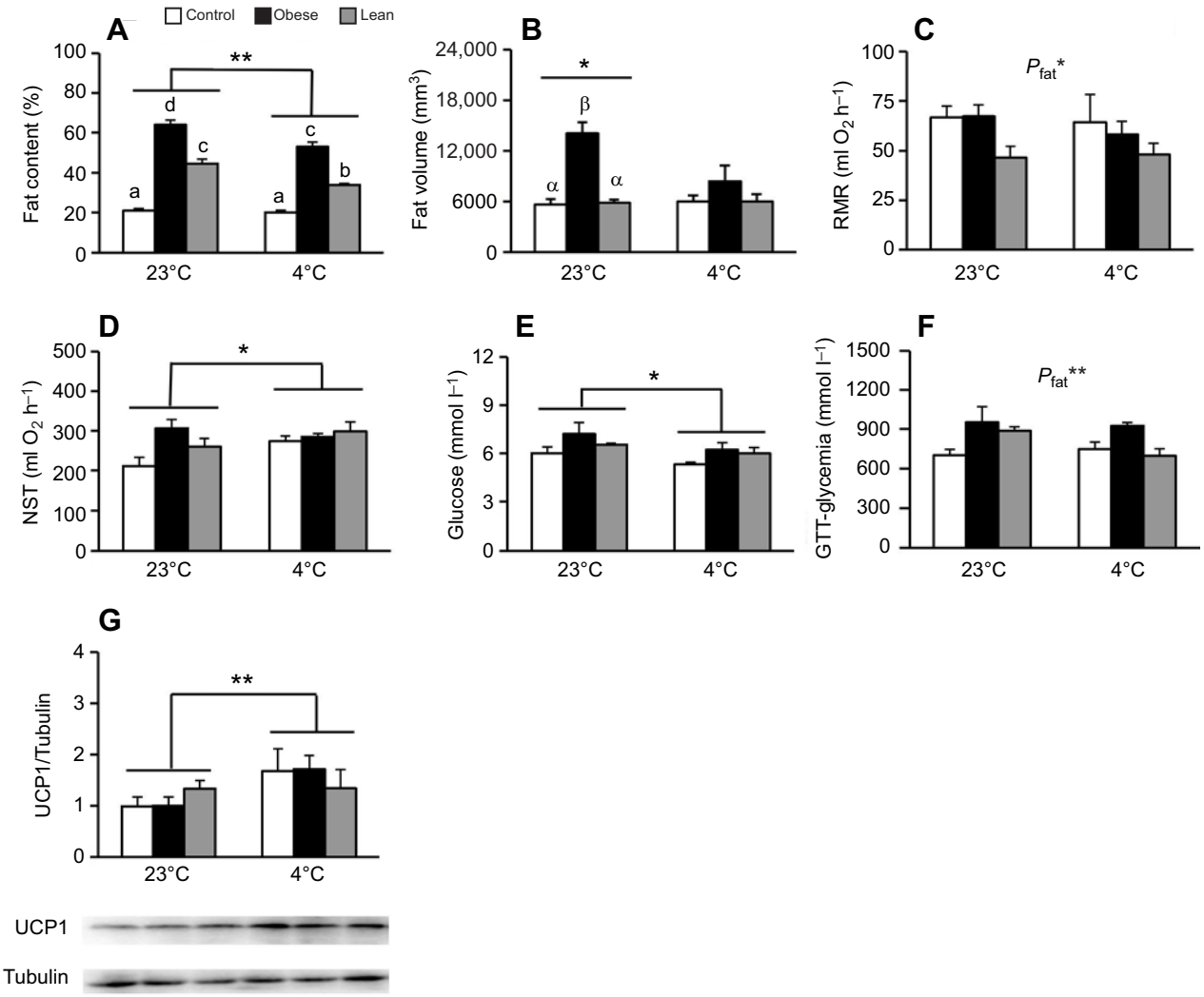

Fig. 2. DIO and low temperature exposure alter the energy metabolism of C57BL/6J mice. Effects of DIO and low temperature exposure on (A) fat content, (B) fat volume, (C) resting metabolic rate, (D) non-shivering thermogenesis, (E) fasting glucose concentration in serum, (F) glucose tolerance test-glycemia and (G) the expression of uncoupling protein 1 in C57BL/6J mice. Data are presented as means±s.e.m. Different letters indicate significant between-group differences determined by Tukey's *post hoc* tests (P<0.05). P_{fat}*, significant effect of DIO (P<0.05). *P<0.05, **P<0.01.

Expression of TRPs

No group difference was found in protein expression levels of TRPA1 and TRPM8 in BAT (Fig. 4A,B). However, in the small intestine, TRPA1 expression was affected by fat ($F_{2,33}$=14.570, P<0.01; Fig. 4C), and when mice were challenged with low temperature exposure, TRPM8 expression levels declined ($F_{1,33}$=5.530, P<0.05; Fig. 4D).

Diversity and composition of gut microbiota and metabolites

Gut microbiota

The OTU-level rarefaction curve of Goods coverage across all samples reached stable values (Fig. S1A), showing that most of the gut microbial diversity had already been captured in our study. As shown in Fig. 5A, the Shannon index showed a significant difference among the six groups ($F_{2,33}$=6.700, P<0.01). The control mice had a higher Shannon index (α-diversity) than the obese and the lean mice ($F_{2,33}$=14.014, P<0.001), but T_a did not significantly affect α-diversity ($F_{1,33}$=3.980, P=0.054). For β-diversity, analysis based on unweighted UniFrac distance (ANOSIM, r=0.35, P=0.001; Fig. 5B) and weighted UniFrac distance (ANOSIM, r=0.32, P=0.001; Fig. 5C) showed significant differences among the six experimental groups. The samples in the control groups (4°C and 23°C) were clustered together, while the other four groups were also clustered together (Fig. 5B,C). Further, the effect of high-fat food was significant (ANOSIM, unweighted: r=0.249, P=0.002; weighted: r=0.251, P=0.001), but that of temperature was not (ANOSIM, unweighted: r=0.016, P=0.232; weighted: r=0.008, P=0.445). The microbial community structures between the 23°C–control group and the 4°C–control group were similar (Fig. 5D). We observed differences in OTU abundance at the phylum level in Bacteroidetes, Proteobacteria and Firmicutes between high-fat content (obese and lean groups) and normal-fat content (control groups) (Fig. 5G,I,J). At the phylum level, the proportions of Firmicutes significantly increased and Bacteroidetes decreased in the obese and lean groups at different temperatures. Actinobacteria (P=0.014) and TM7 (P=0.010) phyla were significantly affected by T_a (Fig. 5F,K). To assess differences in microbial communities affected by fat and T_a, we applied the LEfSe method with an LDA score >2 (Fig. 5E). The results identified 26 and 23 discriminative features in the microbiota of the control and obese groups, respectively, and 29 in the lean group. Fat content (obese and lean groups) significantly augmented the levels of *Oscillospira*,

Journal of Experimental Biology (2020) 223, jeb218974. doi:10.1242/jeb.218974

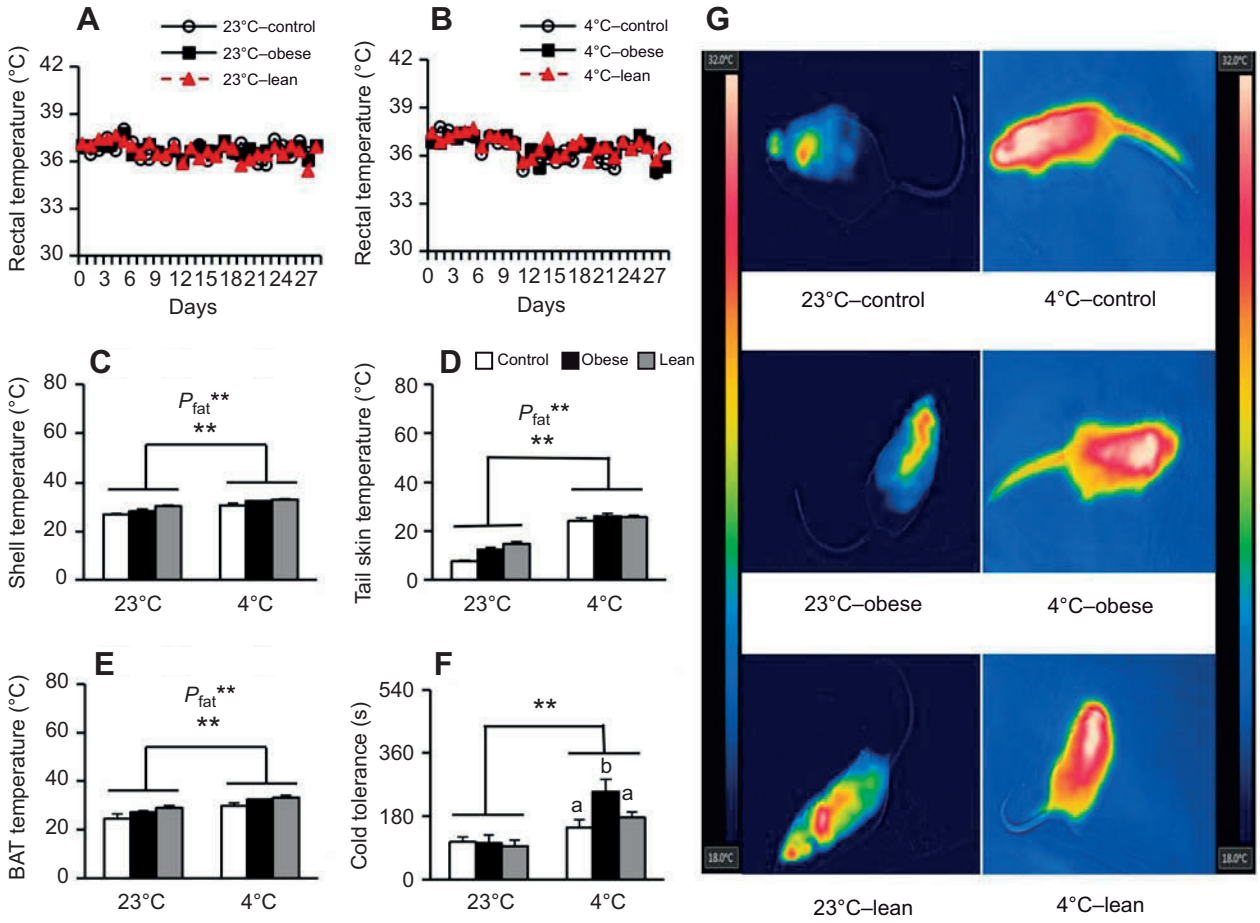

Fig. 3. DIO and low temperature exposure alter the body temperature and cold tolerance of C57BL/6J mice. Effects of DIO and low temperature exposure on (A,B) rectal temperature, (C) shell temperature, (D) tail skin temperature, (E) BAT skin temperature and (F) cold tolerance in C57BL/6J mice. (G) The photos of C57BL/6J mice infrared imaging at 4°C and 23°C. Data are presented as means±s.e.m. Different letters indicate significant between-group differences determined by Tukey's *post hoc* tests (P<0.05). P_{fat}**, significant effect of DIO (P<0.01). **P<0.01.

[*Ruminococcus*], *Lactococcus* and *Christensenella* at the genus level when compared with control groups at different temperatures (Fig. 6B-D,F), but diminished the levels of *Prevotella*, *Odoribacter* and *Lactobacillus* (Fig. 6E,H,I). If only the effect of temperature was considered, we found that the abundance of *Adlercreutzia* (P=0.025; Fig. 6A), [*Ruminococcus*] (P=0.011; Fig. 6C), *Prevotella* (P=0.032; Fig. 6E) and *Christensenella* (P=0.005; Fig. 6F) differed at 4°C and 23°C. The KEGG analysis indicated that the gut microbiota in the obese and lean groups was significantly different in lipid metabolism compared with the control groups (Table S1).

Metabolites

The total concentration of SCFAs in the control groups was slightly higher than in the obese and the lean groups (Fig. 7A). Isovaleric acid and valeric acid levels were significantly affected by fat ($F_{2,33}$=31.67, 25.27, respectively; both P<0.01). Control groups had lower isovaleric acid and valeric acid than the obese and lean groups, which did not differ from each other (Fig. 7B).

NA concentration in the hypothalamus and small intestine

The levels of NA in the hypothalamus were significantly increased by low T_a ($F_{1,33}$=5.452, P<0.05), but not by fat or the fat–T_a interaction ($F_{2,33}$=1.502, 0.790, respectively; both P>0.05; Fig. 8A). The concentration of NA in the small intestine was affected by fat ($F_{1,33}$=9.376, P<0.01), but not by T_a or the fat–T_a interaction ($F_{2,33}$=1.969, 2.497, respectively; both P>0.05; Fig. 8B).

DISCUSSION

In the present study, mice under a low ambient temperature showed significant increases in GEI, but decreases in total body mass gain and body fat content in comparison with their control counterparts. As low temperature exposure causes rapid increases in heat dissipation and thermogenesis, less energy is available for fat deposition, leading to the low temperature-attenuated DIO. Indeed, our data illustrate low temperature-augmented increases in glucose and lipid metabolism. Low temperature exposure not only increased NST and UCP1 expression in the interscapular BAT, but also elevated NA content in the hypothalamus. Increased NA activity in the hypothalamus and in BAT by cold stress are implicated in regulating sympathetic outflow in rats (Gotoh and Smythe, 1991). Thus, our data provide further evidence to support the notion that low temperature-enhanced thermogenesis capacity involves the activation of BAT thermogenesis by participation of hypothalamic NA.

One interesting finding is that although a significant effect of the fat–T_a interaction on GEI was found, obese and lean groups did not increase their GEI during low temperature exposure. One possibility is that the obese and lean groups tended to utilize adipose tissues to meet their energy demand during low temperature exposure. This is

Journal of Experimental Biology (2020) 223, jeb218974. doi:10.1242/jeb.218974

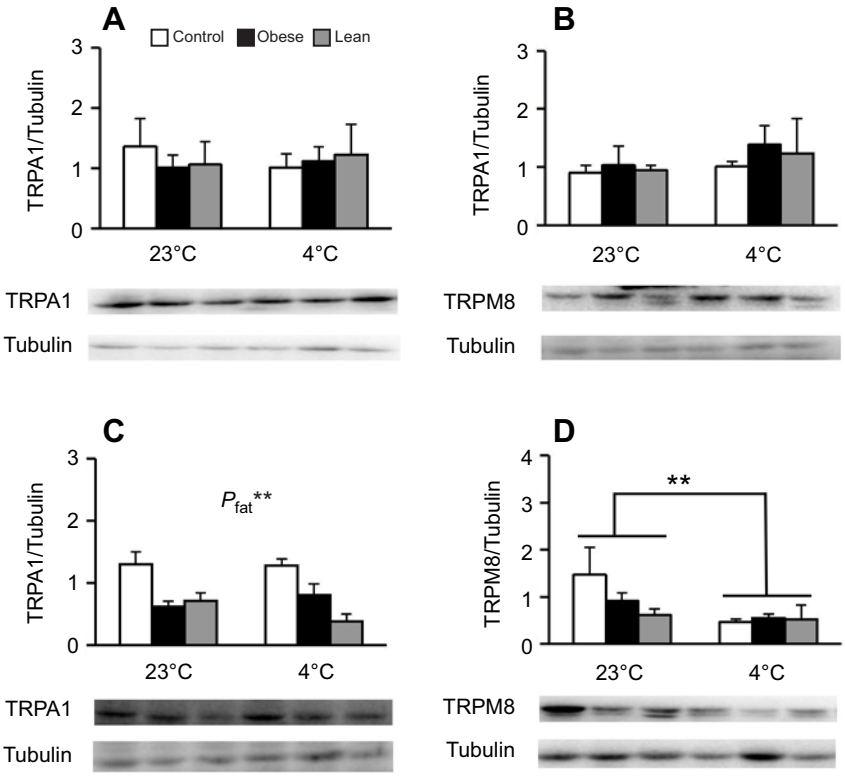

Fig. 4. Expression of TRPA1 and TRPM8 in C57BL/6J mice. Effects of DIO and low temperature exposure on the expression of (A) TRPA1 and (B) TRPM8 in BAT, and the expression of (C) TRPA1 and (D) TRPM8 in the small intestine of C57BL/6J mice. Data are presented as means±s.e.m. Different letters indicate significant between-group differences determined by Tukey's *post hoc* tests (P<0.05). P_{fat}**, significant effect of DIO (P<0.01). **P<0.01.

supported by our data showing an overall decrease in fat content during low temperature exposure in mice. Alternatively, adipose tissue has good thermal insulation properties, so the obese and lean groups with higher fat content can protect themselves from low temperature without additional heat production. This is also supported by our data showing decreased RMR in obese and lean mice and no changes in fat content between the two control groups. It is possible that control and obese mice had different energy utilization strategies when they were exposed to the low ambient temperature.

DIO mice with metabolic dysfunction can progress to a status of passive fat accumulation, leading to body mass gain. The increase in fat content is also a plausible causal factor of insulin resistance in DIO mice (Belfiore et al., 1979). However, in our study, the obese groups showed reduced GEI without significant increases in RMR (compared with the control groups). We speculate that the low energy demand of obese mice is due to the lower mass-specific metabolic rate (calculated as the ratio between RMR and body mass; energy expenditure) and the dry mass of digestive organs (energy expending organs; Table S1). These data are supported by data from a previous study showing that DIO striped hamsters did not change energy intake, but decreased BMR (Shi et al., 2017).

TRPM8 is known for its central role in low temperature detection (Colburn et al., 2007; Señarís et al., 2018), although the expression of TRPM8 in the mouse small intestine remains controversial (Penuelas et al., 2007; Zhang et al., 2004). Our data show that chronic low temperature exposure resulted in a significant decrease in TRPM8 expression in the small intestine, with a drop in rectal temperature (~0.9°C) and an increase in cold tolerance. It has been suggested that TRPM8 may play a role in thermoregulation. For example, although wild-type mice display a strong avoidance of cold environments, this behavior is blunted in TRPM8-deficient mice (Bautista et al., 2007). TRPM8-deficient mice also show an increase in tail heat loss and a fall in core body temperature (~0.7°C), leading to hypothermia (Reimúndez et al., 2018). It has also been demonstrated that deletion of TRPM8 leads to an increase in food intake in mice (Reimúndez et al., 2018). This is supported by our data showing that low temperature-related decreases in TRPM8 expression in the small intestine were associated with an increased GEI. Nevertheless, the role of TRPM8 in food intake/digestion and thermoregulation during low temperature exposure needs to be studied further.

TRPA1 channels are located in the gut and other tissues (Fothergill et al., 2016). Data have shown that TRPA1 can attenuate spontaneous neurogenic contractions and transit of the colon (Poole et al., 2011). Pharmacological activation of TRPA1 can reduce energy intake and ghrelin secretion, delay gastric emptying, and increase insulin release (Ahn et al., 2014; Cao et al., 2012; Señarís et al., 2018). These data indicate that activation of enterocyte TRPA1 has the potential to impede nutrient absorption and obesity (Fothergill et al., 2016). However, our data show that DIO was associated with decreased TRPA1 expression in the small intestine. At the moment, we can only speculate that there might be a disassociation between the amount of TRPA1 and its function. As a thermosensitive channel, TRPA1 can also be activated by fatty acids – especially for animals receiving high-fat food (Terada et al., 2011). TRPA1 activation can induce adrenaline secretion via sensory nerve activation and ultimately inhibit fat deposition by increasing thermogenesis and energy expenditure (Iwasaki et al., 2008; Terada et al., 2011; Watanabe and Terada, 2015). In our obese mice, TRPA1 expression in the small intestine was reduced, but NA content changed in the opposite direction. NA in the small intestine can be transmitted as a signal molecule to gut microbes, which, in turn, release SCFAs to form a feedback loop (Bo et al., 2019). Therefore, it is possible that the low levels of TRPA1 in the small intestine had a higher activation rate and still played a role in mediating low temperature-attenuated DOI. This speculation needs to be examined in further studies.

Journal of Experimental Biology (2020) 223, jeb218974. doi:10.1242/jeb.218974

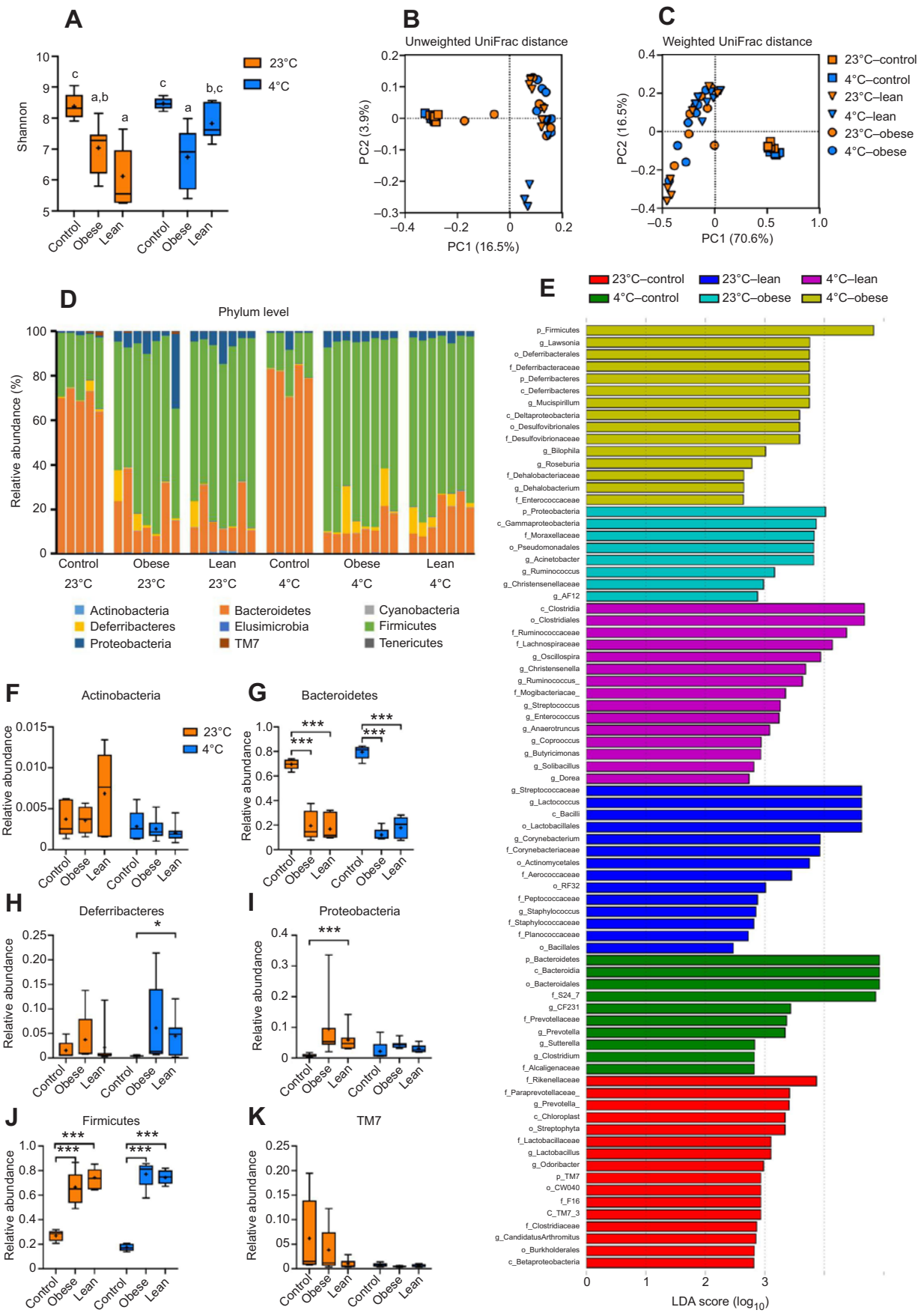

Fig. 5. See next page for legend.

Journal of Experimental Biology (2020) 223, jeb218974. doi:10.1242/jeb.218974

Fig. 5. DIO and low temperature exposure alter the diversity and composition of fecal microbiota at the phylum level. (A) Shannon index (α-diversity) of gut microbiota. (B,C) Principal coordinate analysis (PCoA) plots based on (B) unweighted UniFrac distance and (C) weighted UniFrac distance. (D) Relative abundance at the phylum level in the fecal microbiota community of the six groups. (E) Differential bacterial taxonomy selected by LEfSe analysis with LDA score >2 in the fecal microbiota community of the six groups. (F–K) Relative abundance of (F) Actinobacteria, (G) Bacteroidetes, (H) Deferribacteres, (I) Proteobacteria, (J) Firmicute and (K) TM7 in the fecal microbiota community of the six groups at phylum level. In G to L, the black crosses indicate the means of data. Different letters indicate significant between-group differences determined by Tukey's *post hoc* tests (P<0.05). *P<0.05; ***P<0.001.

Gut microbiota could be linked to the development of obesity and related comorbidities (Moreno-Indias et al., 2016). Our data show that the abundance of Firmicutes was significantly increased, but that of Bacteroidetes was decreased at the phyla level in DIO mice. Previous studies have demonstrated that an increase in the ratio of Firmicutes/Bacteroidetes was positively correlated with body fat content (Ley et al., 2005; Turnbaugh et al., 2008). Bacteria belonging to Firmicutes are enriched in mice with a high-fat diet and are usually associated with obesity (Turnbaugh et al., 2008). Conversely, bacteria belonging to Bacteroidetes are usually higher in control groups and are associated with leanness (Goodrich et al., 2014). We also observed that the abundance of *Oscillospira*, [*Ruminococcus*], *Lactococcus* and *Christensenella* at the genus level increased, and the abundance of *Prevotella*, *Odoribacter* and *Lactobacillus* at the genus level decreased in DIO mice, which is consistent with results from previous studies in rats and mice (Lin et al., 2019; Tung et al., 2018). In addition, Spearman's correlation analyses have negatively linked the abundance of *Oscillospira* with most metabolic parameters (Li et al., 2019b). Although our data support the notion that alterations in these bacteria may serve as the markers of morbid obesity, it should not be ignored that group differences in dietary composition/intake may also be attributing to differences seen in fecal bacteria composition between the obese and non-obese groups in our present study. Changes in gut microbiota cause changes in SCFAs. Evidence indicates that isovaleric acid (42.11%) increases, while valeric acid (23.92%) decreases in

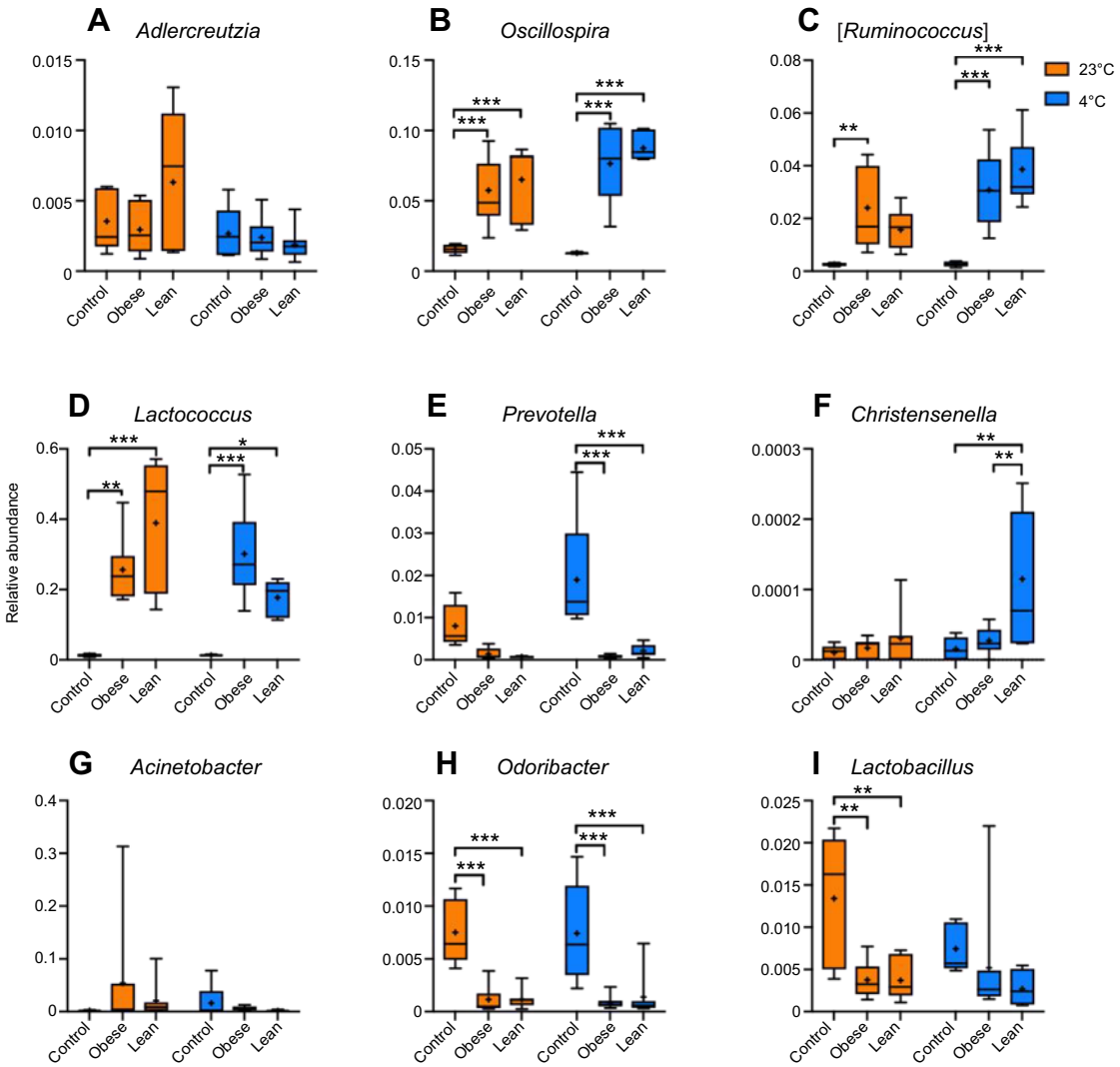

Fig. 6. DIO and low temperature exposure alter the diversity and composition of fecal microbiota at the genus level. Relative abundance of (A) *Adlercreutzia*, (B) *Oscillospira*, (C) [*Ruminococcus*], (D) *Lactococcus*, (E) *Prevotella*, (F) *Christensenlla*, (G) *Acinetobacter*, (H) *Odoribacter* and (I) *Lactobacillus* in the fecal microbiota community of the six groups at genus level. Black crosses indicate the means of data. *P<0.05; **P<0.01; ***P<0.001.

Journal of Experimental Biology (2020) 223, jeb218974. doi:10.1242/jeb.218974

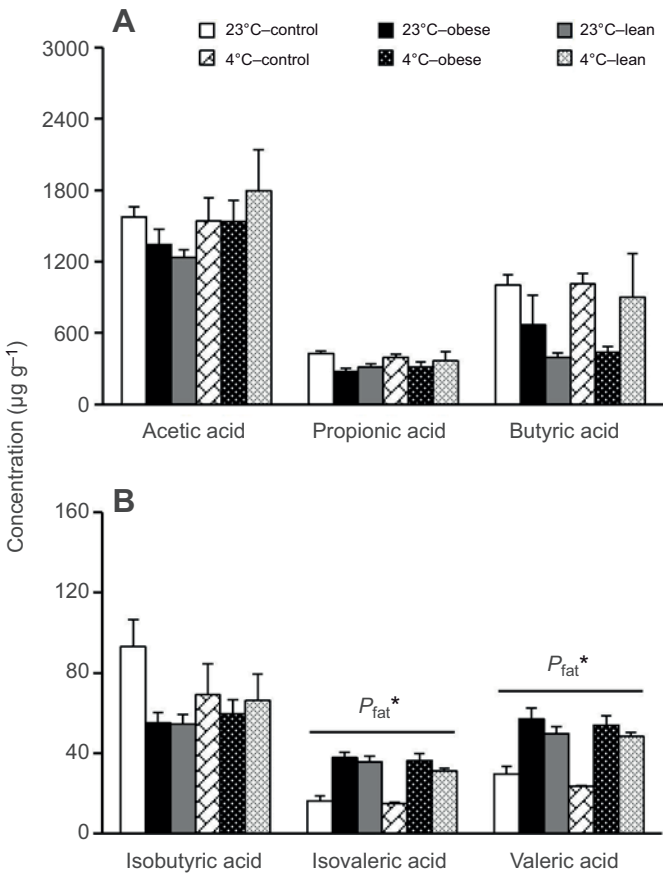

Fig. 7. Effects of DIO on short-chain fatty acid concentration in feces of C57BL/6J mice. Data are presented as means±s.e.m. P_{fat}*, significant effect of DIO (P<0.01).

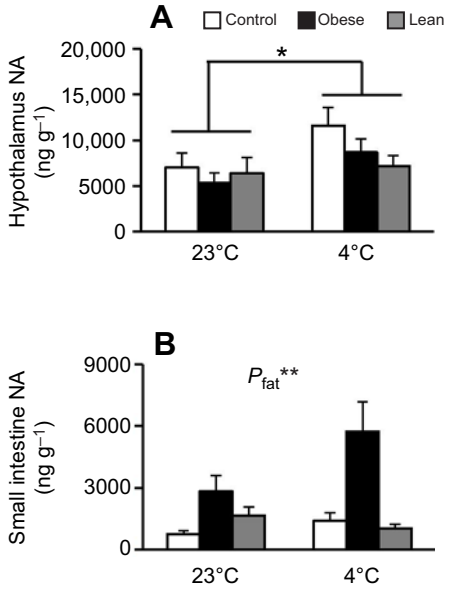

Fig. 8. Noradrenaline (NA) levels in C57BL/6J mice. Effects of DIO and low temperature exposure on the concentration of NA in (A) the hypothalamus and (B) the small intestine of C57BL/6J mice. Data are presented as means ±s.e.m. P_{fat}**, significant effect of DIO (P<0.01). *P<0.05.

colon contents in obese mice (Li et al., 2018). In the present study, isovaleric acid and valeric acid in fecal samples were significantly increased in both the obese and the lean groups. Fat–T_a interactions also influenced gut microbiota structure of mice. The α-diversity of gut microbiota decreased in DIO mice, which was conserved by low temperature exposure. Consistent with the study of Zietak et al. (2016), we identified that the abundance of Actinobacteria and TM7 at the phylum level were decreased when mice were exposed to low temperature, suggesting that the changes in these bacteria may contribute to the cold-induced phenotype and inhibit adiposity in mice (Zietak et al., 2016). The mechanism of gut microbiota influencing adiposity may include modulation of NA concentrations (Bo et al., 2019). NA can alleviate obesity through increased thermogenesis (Gotoh and Smythe, 1991).

Conclusions

In the present study, we found that BAT thermogenesis was associated with increased N7A concentrations in the hypothalamus and enhanced TRPM8 expression in the small intestine during low temperature exposure. Energy intake and TRPA1 in the small intestine were reduced, and NA in the small intestine was increased in DIO mice. Further, we found that ambient temperature and DIO can interact in altering the composition and diversity of gut microbiota. Together, our data indicate that low temperature-attenuated DIO may be mediated by changes in BAT thermogenesis, TRP (TRPA1 and TRPM8) activity, and gut microbiota composition, and through their interactions. In addition, we suggest that *Oscillospira*, [*Ruminococcus*], *Lactococcus* and *Christensenella* at the genus level are potential bacterial markers related to morbid obesity, while *Prevotella*, *Odoribacter* and *Lactobacillus* at the genus level are potential bacterial markers that impede obesity. TRPM8 and TRPA1 may also serve as potential therapeutic targets for preventing/treating obesity and its related metabolic disorders.

Acknowledgements

We thank all the members of Animal Physiological Ecology Group of the Institute of Zoology, Chinese Academy of Sciences, for their helpful discussion. J.W. thanks Qing-gang Qiao for his encouragement.

Competing interests

The authors declare no competing or financial interests.

Author contributions

Methodology: J.W., T.B.; Software: T.B.; Data curation: J.W.; Writing - original draft: J.W.; Writing - review & editing: J.W., X.Y.Z., Z.W., D.H.W.; Supervision: D.H.W.; Project administration: X.Y.Z., D.H.W.; Funding acquisition: D.H.W.

Funding

This work was supported by the National Natural Science Foundation of China (grants 31970417 and 31772461 to D.H.W., and 31770440 to X.Y.Z.).

Supplementary information

Supplementary information available online at
http://jeb.biologists.org/lookup/doi/10.1242/jeb.218974.supplemental

References

Ahn, J., Lee, H., Im, S. W., Jung, C. H. and Ha, T. Y. (2014). Allyl isothiocyanate ameliorates insulin resistance through the regulation of mitochondrial function. *J. Nutr. Biochem.* **25**, 1026-1034. doi:10.1016/j.jnutbio.2014.05.006

Bachman, E. S., Harveen, D., Chen-Yu, Z., Saverio, C., Bianco, A. C., Kobilka, B. K. and Lowell, B. B. (2002). betaAR signaling required for diet-induced thermogenesis and obesity resistance. *Science* **297**, 843-845. doi:10.1126/science.1073160

Bäckhed, F., Manchester, J. K., Semenkovich, C. F. and Gordon, J. I. (2007). Mechanisms underlying the resistance to diet-induced obesity in germ-free mice. *Proc. Natl. Acad. Sci. USA* **104**, 979-984. doi:10.1073/pnas.0605374104

Barbatelli, G., Murano, I., Madsen, L., Hao, Q., Jimenez, M., Kristiansen, K., Giacobino, J. P., De Matteis, R. and Cinti, S. (2010). The emergence of cold-

induced brown adipocytes in mouse white fat depots is determined predominantly by white to brown adipocyte transdifferentiation. *Am. J. Physiol. Endocrinol. Metab.* **298**, E1244-E1253. doi:10.1152/ajpendo.00600.2009

Bautista, D. M., Siemens, J., Glazer, J. M., Tsuruda, P. R., Basbaum, A. I., Stucky, C. L., Jordt, S.-E. and Julius, D. (2007). The menthol receptor TRPM8 is the principal detector of environmental cold. *Nature* **448**, 204-208. doi:10.1038/nature05910

Belfiore, F., Iannello, S. and Rabuazzo, A. M. (1979). Insulin resistance in obesity: a critical analysis at enzyme level. *Int. J. Obes.* **3**, 301-323.

Bo, T.-B., Zhang, X.-Y., Wen, J., Deng, K., Qin, X.-W. and Wang, D.-H. (2019). The microbiota–gut–brain interaction in regulating host metabolic adaptation to cold in male Brandt's voles (*Lasiopodomys brandtii*). *ISME J.* **13**, 3037-3053. doi:10.1038/s41396-019-0492-y

Bödding, M., Wissenbach, U. and Flockerzi, V. (2007). Characterisation of TRPM8 as a pharmacophore receptor. *Cell. Calcium.* **42**, 618-628. doi:10.1016/j.ceca.2007.03.005

Cannon, B. and Nedergaard, J. (2004). Brown adipose tissue: function and physiological significance. *Physiol. Rev.* **84**, 277-359. doi:10.1152/physrev.00015.2003

Cao, D.-S., Zhong, L., Hsieh, T.-H., Abooj, M., Bishnoi, M., Hughes, L. and Premkumar, L. S. (2012). Expression of transient receptor potential ankyrin 1 (TRPA1) and its role in insulin release from rat pancreatic beta cells. *PLoS ONE* **7**, e38005. doi:10.1371/journal.pone.0038005

Chevalier, C., Stojanović, O., Colin, D. J., Suarez-Zamorano, N., Tarallo, V., Veyrat-Durebex, C., Rigo, D., Fabbiano, S., Stevanović, A., Hagemann, S. et al. (2015). Gut microbiota orchestrates energy homeostasis during cold. *Cell.* **163**, 1360-1374. doi:10.1016/j.cell.2015.11.004

Colburn, R. W., Lubin, M. L., Stone, D. J., , Jr, Wang, Y., Lawrence, D., D'Andrea, M. R., Brandt, M. R., Liu, Y., Flores, C. M. and Qin, N. (2007). Attenuated cold sensitivity in TRPM8 null mice. *Neuron* **54**, 379-386. doi:10.1016/j.neuron.2007.04.017

Fothergill, L. J., Callaghan, B., Rivera, L. R., Lieu, T. M., Poole, D. P., Cho, H. J., Bravo, D. M. and Furness, J. B. (2016). Effects of food components that activate TRPA1 receptors on mucosal ion transport in the mouse intestine. *Nutrients* **8**, 623. doi:10.3390/nu8100623

Goodrich, J. K., Waters, J. L., Poole, A. C., Sutter, J. L., Koren, O., Blekhman, R., Beaumont, M., Van Treuren, W., Knight, R., Bell, J. T. et al. (2014). Human genetics shape the gut microbiome. *Cell* **159**, 789-799. doi:10.1016/j.cell.2014.09.053

Gotoh, M. and Smythe, G. A. (1991). Effects of intracerebroventricularly administered neostigmine on sympathetic neural activities of peripheral tissues in rats. *Brain Res.* **548**, 326-328. doi:10.1016/0006-8993(91)91142-N

Heldmaier, G. (1971). Nonshivering thermogenesis and body size in mammals. *J. Comp. Physiol.* **73**, 222-248.

Hoffstaetter, L. J., Bagriantsev, S. N. and Gracheva, E. O. (2018). TRPs et al.: a molecular toolkit for thermosensory adaptations. *Pflugers. Arch.* **470**, 745-759. doi:10.1007/s00424-018-2120-5

Iwasaki, Y., Tanabe, M., Kobata, K. and Watanabe, T. (2008). TRPA1 agonists—allyl isothiocyanate and cinnamaldehyde—induce adrenaline secretion. *Biosci. Biotechnol. Biochem.* **72**, 2608-2614. doi:10.1271/bbb.80289

Ley, R. E., Backhed, F., Turnbaugh, P., Lozupone, C. A., Knight, R. D. and Gordon, J. I. (2005). Obesity alters gut microbial ecology. *Proc. Natl. Acad. Sci. USA* **102**, 11070-11075. doi:10.1073/pnas.0504978102

Ley, R. E., Turnbaugh, P. J., Klein, S. and Gordon, J. I. (2006). Microbial ecology: human gut microbes associated with obesity. *Nature* **444**, 1022-1023. doi:10.1038/4441022a

Li, H. (2017). TRP channel classification. *Adv. Exp. Med. Biol.* **976**, 1-8. doi:10.1007/978-94-024-1088-4_1

Li, Y., Ouyang, P. L., Dan, Q. U., Jiang, R. and Song, L. H. (2018). Effects of phytosterol ester on short-chain fatty acids in colon content of rats fed a high fat diet. *Sci. Technol. Food Industry* **39**, 292-297.

Li, B., Li, L., Li, M., Lam, S. M., Wang, G., Wu, Y., Zhang, H., Niu, C., Zhang, X., Liu, X. et al. (2019a). Microbiota depletion impairs thermogenesis of brown adipose tissue and browning of white adipose tissue. *Cell Rep.* **26**, 2720-2737.e5. doi:10.1016/j.celrep.2019.02.015

Li, X., Wang, H., Wang, T., Zheng, F., Wang, H. and Wang, C. (2019b). Dietary wood pulp-derived sterols modulation of cholesterol metabolism and gut microbiota in high-fat-diet-fed hamsters. *Food. Funct.* **10**, 775-785. doi:10.1039/C8FO02271B

Lin, H., An, Y., Tang, H. and Wang, Y. (2019). Alterations of bile acids and gut microbiota in obesity induced by high fat diet in rat model. *J. Agric. Food. Chem.* **67**, 3624-3632. doi:10.1021/acs.jafc.9b00249

Ma, S., Yu, H., Zhao, Z., Luo, Z., Chen, J., Ni, Y., Jin, R., Ma, L., Wang, P., Zhu, Z. et al. (2012). Activation of the cold-sensing TRPM8 channel triggers UCP1-dependent thermogenesis and prevents obesity. *J. Molecul. Cell Biol.* **4**, 88-96. doi:10.1093/jmcb/mjs001

Magoč, T. and Salzberg, S. L. (2011). Flash: fast length adjustment of short reads to improve genome assemblies. *Bioinformatics* **27**, 2957-2963. doi:10.1093/bioinformatics/btr507

Moreno-Indias, I., Sánchez-Alcoholado, L., García-Fuentes, E., Cardona, F., Queipo-Ortuño, M. I. and Tinahones, F. J. (2016). Insulin resistance is associated with specific gut microbiota in appendix samples from morbidly obese patients. *Am. J. Transl. Res.* **8**, 5672-5684.

Nilius, B. and Owsianik, G. (2011). The transient receptor potential family of ion channels. *Genome. Biol.* **12**, 218. doi:10.1186/gb-2011-12-3-218

Nudel, J. and Sanchez, V. M. (2019). Surgical management of obesity. *Metabolism* **92**, 206-216. doi:10.1016/j.metabol.2018.12.002

Penuelas, A., Tashima, K., Tsuchiya, S., Matsumoto, K., Nakamura, T., Horie, S. and Yano, S. (2007). Contractile effect of TRPA1 receptor agonists in the isolated mouse intestine. *Eur. J. Pharmacol.* **576**, 143-150. doi:10.1016/j.ejphar.2007.08.015

Poole, D. P., Pelayo, J. C., Cattaruzza, F., Kuo, Y. M., Gai, G., Chiu, J. V., Bron, R., Furness, J. B., Grady, E. F. and Bunnett, N. W. (2011). Transient receptor potential ankyrin 1 is expressed by inhibitory motoneurons of the mouse intestine. *Gastroenterology* **141**, 565-575.e4. doi:10.1053/j.gastro.2011.04.049

Ravussin, Y., Xiao, C., Gavrilova, O. and Reitman, M. L. (2014). Effect of intermittent cold exposure on brown fat activation, obesity, and energy homeostasis in mice. *PLoS ONE* **9**, e85876. doi:10.1371/journal.pone.0085876

Reimúndez, A., Fernández-Peña, C., García, G., Fernández, R., Ordás, P., Gallego, R., Pardo-Vazquez, J. L., Arce, V., Viana, F. and Señarís, R. (2018). Deletion of the cold thermoreceptor TRPM8 increases heat loss and food intake leading to reduced body temperature and obesity in mice. *J. Neurosci.* **38**, 3643-3656. doi:10.1523/JNEUROSCI.3002-17.2018

Romieu, I., Dossus, L., Barquera, S., Blottière, H. M., Franks, P. W., Gunter, M., Hwalla, N., Hursting, S. D., Leitzmann, M., Margetts, B. et al. (2017). Energy balance and obesity: what are the main drivers? *Cancer Causes Control* **28**, 247-258. doi:10.1007/s10552-017-0869-z

Rossato, M., Granzotto, M., Macchi, V., Porzionato, A., Petrelli, L., Calcagno, A., Vencato, J., De Stefani, D., Silvestrin, V., Rizzuto, R. et al. (2014). Human white adipocytes express the cold receptor TRPM8 which activation induces UCP1 expression, mitochondrial activation and heat production. *Mol. Cell. Endocrinol.* **383**, 137-146. doi:10.1016/j.mce.2013.12.005

Rothwell, N. J. and Stock, M. J. (1979). Regulation of energy balance in two models of reversible obesity in the rat. *J. Comp. Physiol. Psychol.* **93**, 1024-1034. doi:10.1037/h0077631

Saito, M., Yoneshiro, T. and Matsushita, M. (2015). Food ingredients as anti-obesity agents. *Trends. Endocrinol. Metab.* **26**, 585-587. doi:10.1016/j.tem.2015.08.009

Señarís, R., Ordás, P., Reimúndez, A. and Viana, F. (2018). Mammalian cold TRP channels: impact on thermoregulation and energy homeostasis. *Pflugers. Arch.* **470**, 761-777. doi:10.1007/s00424-018-2145-9

Shi, L.-L., Fan, W.-J., Zhang, J.-Y., Zhao, X.-Y., Tan, S., Wen, J., Cao, J., Zhang, X.-Y., Chi, Q.-S., Wang, D.-H. et al. (2017). The roles of metabolic thermogenesis in body fat regulation in striped hamsters fed high-fat diet at different temperatures. *Comp. Biochem. Physiol. A Mol. Integr. Physiol.* **212**, 35-44. doi:10.1016/j.cbpa.2017.07.002

Song, K., Wang, H., Kamm, G. B., Pohle, J., Reis, F. C., Heppenstall, P., Wende, H. and Siemens, J. (2016). The TRPM2 channel is a hypothalamic heat sensor that limits fever and can drive hypothermia. *Science* **353**, 1393-1398. doi:10.1126/science.aaf7537

Suárez-Zamorano, N., Fabbiano, S., Chevalier, C., Stojanović, O., Colin, D. J., Stevanović, A., Veyrat-Durebex, C., Tarallo, V., Rigo, D., Germain, S. et al. (2015). Microbiota depletion promotes browning of white adipose tissue and reduces obesity. *Nat. Med.* **21**, 1497-1501. doi:10.1038/nm.3994

Terada, Y., Narukawa, M. and Watanabe, T. (2011). Specific hydroxy fatty acids in royal jelly activate TRPA1. *J. Agric. Food. Chem.* **59**, 2627-2635. doi:10.1021/jf1041646

Tremaroli, V. and Bäckhed, F. (2012). Functional interactions between the gut microbiota and host metabolism. *Nature* **489**, 242-249. doi:10.1038/nature11552

Tung, Y.-C., Chang, W.-T., Li, S., Wu, J.-C., Badmeav, V., Ho, C.-T. and Pan, M.-H. (2018). Citrus peel extracts attenuated obesity and modulated gut microbiota in mice with high-fat diet-induced obesity. *Food. Funct.* **9**, 3363-3373. doi:10.1039/C7FO02066J

Turnbaugh, P. J., Bäckhed, F., Fulton, L. and Gordon, J. I. (2008). Diet-induced obesity is linked to marked but reversible alterations in the mouse distal gut microbiome. *Cell. Host. Microbe* **3**, 213-223. doi:10.1016/j.chom.2008.02.015

Uchida, K., Dezaki, K., Yoneshiro, T., Watanabe, T., Yamazaki, J., Saito, M., Yada, T., Tominaga, M. and Iwasaki, Y. (2017). Involvement of thermosensitive TRP channels in energy metabolism. *J. Physiol. Sci.* **67**, 549-560. doi:10.1007/s12576-017-0552-x

Vay, L., Gu, C. and McNaughton, P. A. (2012). The thermo-TRP ion channel family: properties and therapeutic implications. *Br. J. Pharmacol.* **165**, 787-801. doi:10.1111/j.1476-5381.2011.01601.x

Watanabe, T. and Terada, Y. (2015). Food compounds activating thermosensitive TRP channels in Asian herbal and medicinal foods. *J. Nutr. Sci. Vitaminol.* **61**, S86-S88. doi:10.3177/jnsv.61.S86

Yoo, H. S., Qiao, L., Bosco, C., Leong, L.-H., Lytle, N., Feng, G.-S., Chi, N.-W. and Shao, J. (2014). Intermittent cold exposure enhances fat accumulation in mice. *PLoS ONE* **9**, e96432. doi:10.1371/journal.pone.0096432

Zhang, L., Jones, S., Brody, K., Costa, M. and Brookes, S. J. H. (2004). Thermosensitive transient receptor potential channels in vagal afferent neurons of the mouse. *Am. J. Physiol.* **286**, G983-G991. doi:10.1152/ajpgi.00441.2003

Zhang, X.-Y., Sukhchuluun, G., Bo, T.-B., Chi, Q.-S., Yang, J.-J., Chen, B., Zhang, L. and Wang, D.-H. (2018). Huddling remodels gut microbiota to reduce energy requirements in a small mammal species during cold exposure. *Microbiome* **6**, 103. doi:10.1186/s40168-018-0473-9

Ziętak, M., Kovatcheva-Datchary, P., Markiewicz, L. H., Stahlman, M., Kozak, L. P. and Backhed, F. (2016). Altered microbiota contributes to reduced diet-induced obesity upon cold exposure. *Cell. Metab.* **23**, 1216-1223. doi:10.1016/j.cmet.2016.05.001